Chem Soc Rev

This article was published as part of the

In-situ characterization of heterogeneous catalysts themed issue

Guest editor Bert M. Weckhuysen

Please take a look at the issue 12 2010 table of contents to access other reviews in this themed issue

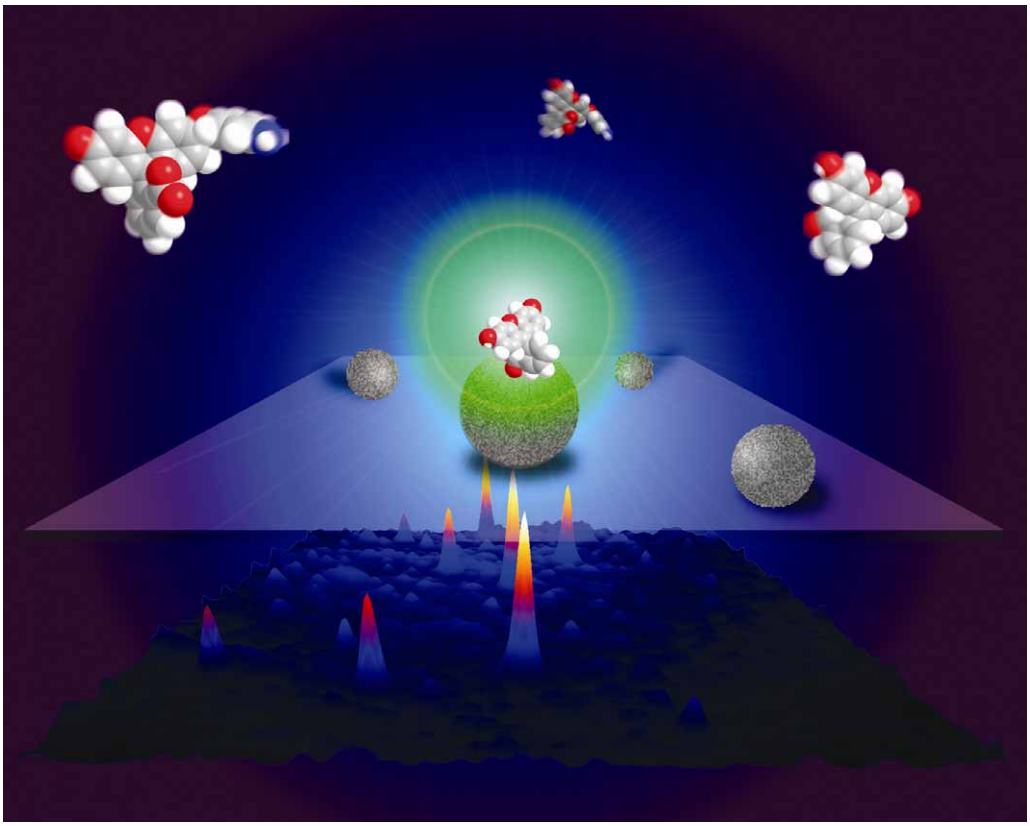

Infrared and Raman imaging of heterogeneous catalysts†

Eli Stavitski and Bert M. Weckhuysen*

Received 3rd August 2010
DOI: 10.1039/c0cs00064g

The miniaturization of *in situ* spectroscopic tools has been recognized as a forefront instrumental development for the characterization of heterogeneous catalysts. With the multitude of micro-spectroscopic methods available fundamental insight into the structure–function relationships of catalytic processes can be obtained. Among these techniques vibrational spectroscopy is one of the most versatile methods and capable to shed insight into the molecular structure of reaction intermediates and products, the chemical state of catalyst materials during reaction as well as the nature of interactions between reactants/intermediates/products and the catalyst surface. In this *tutorial review* we discuss the recent developments in the field of infrared (IR) and Raman micro-spectroscopy and illustrate their potential. Showcase examples include (1) chemical imaging of spatial heterogeneities during catalyst preparation, (2) high-throughput catalyst screening, (3) transport and adsorption phenomena within catalytic solids and (4) reactivity studies of porous oxides, such as zeolites. Finally, new *in situ* spectroscopy tools based on vibrational spectroscopy and their potential in the catalysis domain are discussed.

Introduction

Along the torturous pathway of a heterogeneous catalytic reaction, abstruse chemical transformations occur leading to the formation of unstable and short-living intermediates, whose structures frequently defy the imagination of a chemist.[1] If the final product is the one sought after, these complex reactions are often overlooked as irrelevant to the overall conversion and selectivity or to other industrially important characteristics, such as *e.g.* catalyst stability. However, most scientists are interested in exactly those aspects of a catalytic process as the understanding of the complex factors underlying a catalytic process is key to optimizing a chemical reaction and designing superior catalyst materials, based on a rational catalyst design approach rather than adopting a hit-and-miss strategy.

Since the pioneering work of Eischens and co-workers[2,3] a large number of *in situ* spectroscopy techniques have been

Inorganic Chemistry and Catalysis Group,
Debye Institute for Nanomaterials Science, Utrecht University,
Sorbonnelaan 16, 3584 CA Utrecht, The Netherlands.
E-mail: b.m.weckhuysen@uu.nl; Fax: +31 30 251 1027
† Part of the themed issue covering recent advances in the *in situ* characterization of heterogeneous catalysts.

Eli Stavitski

Dr Eli Stavitski received his PhD in 2006 at the Hebrew University of Jerusalem (Israel) with Prof. Haim Levanon, followed by postdoctoral research at Utrecht University and Delft University of Technology in the Netherlands. In 2008 he received a VENI research award from the Netherlands Organization for Scientific Research. Since October 2010, he is a research associate at the National Synchrotron Light Source, Brookhaven National Laboratory (USA). His research focus is on the development and application of spectroscopic methods to gain molecular understanding of bio- and heterogeneous catalytic systems.

Bert M. Weckhuysen

Bert Weckhuysen (42), a native Belgian, received his master degree from Leuven University (Belgium) in 1991. After finishing his PhD studies under the supervision of Prof. Schoonheydt in 1995, he has worked as a postdoctoral fellow with Prof. Wachs at Lehigh University (USA) and with Prof. Lunsford at Texas A&M University (USA). Weckhuysen has been a full professor of inorganic chemistry and catalysis at Utrecht University since 2000. He has authored over 250 publications in peer-reviewed scientific journals and received several research awards, including the 2006 Gold Medal from the Royal Dutch Chemical Society, the 2007 DECHEMA Award from The Max Buchner Research Foundation (Germany) and the 2009 Netherlands Catalysis and Chemistry Award. Weckhuysen is also the scientific director of the Dutch Research School for Catalysis (NIOK).

introduced in the field of heterogeneous catalysis.[4,5] They have been used to elucidate the intricate catalytic chemistry taking place in *e.g.* porous oxides and supported transition metal oxides. These various powerful methods available range all the way from optical and vibrational spectroscopy (UV-Vis, Raman, IR)[6–8] over magnetic resonance (ESR and NMR)[9,10] to X-ray absorption (EXAFS and XANES)[11] and photoelectron (XPS) spectroscopy.[12] It would not be an exaggeration to say that almost every conceivable characterization tool available has found its way to the field of catalysis to help realizing the above-mentioned scientific ambition of rational catalyst design.

It appears that many scientific challenges pertaining to the understanding of heterogeneous catalysis at a very fundamental level can be insufficiently dealt with the more conventional spectroscopic tools. One of the major limitations is the size of the region of the catalytic samples being probed, or, in other words, the volume of the material excited by electromagnetic radiation and/or the volume from which the radiation is collected. Out of convenience and due to technical restrictions, the spot size in most of the spectroscopic methods is maintained in the range of 0.1–1 cm, which is ideal for sizable (powdered) samples, in, *e.g.*, an *in situ* spectroscopic cell, accommodating self-standing wafers or quartz reactor. Unfortunately, when experiments are carried out in this way, chemical information is obtained from the entire sample, therefore averaging it over whole the population of catalytic sites.[13]

However, fundamental studies in surface science have convincingly demonstrated that distinct areas of the catalytic particles, for instance, crystalline faces of different orientation can exhibit varying catalytic activities and/or selectivities.[14] While model catalysts, such as well-defined metal or metal oxide surfaces, have been successfully employed, the real systems often possess the structural features of nanometres to micrometre-sizes. The 'dream *in situ* spectroscopy instrument' should be able to deliver dynamic information on the different areas of a catalyst material in terms of their structure–performance, thereby providing with a more complete picture of the overall catalytic process.[15,16]

In the past decade several groups have focused their efforts on miniaturization of *in situ* spectroscopic tools. Among the most informative, UV-Vis,[17] fluorescence,[18,19] X-ray micro-spectroscopy[20–23] and NMR[24,25] should be mentioned. Given the progress, it is reasonable to assume that almost every instrument can be sized down, including vibrational spectroscopy.

Vibrational methods are most probably one of the most powerful techniques in the arsenal of the catalysis researcher thanks to the direct chemical information one can extract from IR and Raman spectra.[4,5] They include the nature of a chemical bonding, from which the determination of the chemical structure of the reaction intermediates and products is feasible. In parallel, the state of the catalyst, in terms of chemical composition, hydration degree and redox state can be probed under *in situ* conditions. Moreover, most products causing deactivation of the catalysts, *e.g.* carbonaceous deposits exhibit strong features in both IR and Raman spectra. Notwithstanding the foregoing advantages, every spectroscopist familiar with hands-on implementation of the above characterization methods could name many factors hindering their usability and narrowing down the scope of data obtainable. The most severe among them is the relatively low sensitivity, insufficient time resolution due to the long signal accumulation times and the interference of the gas phase when the experiments are conducted at atmospheric or higher pressures. However, vibrational spectroscopy has proved to be of outstanding importance in heterogeneous catalysis research despite these shortcomings.

In what follows we shortly describe the technical requirements of IR and Raman micro-spectroscopy and review the applications in the field of heterogeneous catalysis reported so far. The review article ends with a perspective on related emerging characterization methods, which have the capacity to bring about unprecedented insight into the function of catalytic systems one step closer.

Instrumentation

After a brief discussion of the merits of miniaturization, we will describe the nuts-and-bolts of the instrumentation for IR and Raman micro-spectroscopy. The arrival of Fourier-transform IR (FT-IR) spectrometers in the early 1970s has irrevocably transformed the field by drastically cutting measurement times; nowadays these machines are the work-horses in nearly every catalytic lab, used extensively for routine catalyst characterization, *in situ* investigation and often for product analysis in gas and/or liquid phases.[6] An FT-IR spectrometer is the basis for the IR microscope, providing both the build-in excitation and detection modules, whether the microscope optics provides the focusing capabilities. Traditional glass or quartz lens-based objectives are not suitable in this case since the IR light is largely absorbed by silica, therefore calling for other designs, such as, for example, an all-reflective objective. Those optical elements, also known as Schwarzschild objectives comprise two concentric spherical mirrors. Interestingly, this focusing arrangement lacks some drawbacks typical for conventional multi-lens objectives, such as material absorption and chromatic aberrations, that is, the focal distance remains constant over a broad spectral range. Another advantage is the relatively large working distance, making it possible to fit, *e.g.*, an *in situ* appliance underneath. On the downside, the numerical aperture value for the commercially available reflective objectives does not exceed 0.6. These values determine the highest attainable spatial resolution to be roughly $2/3\lambda$ with a single objective.[26]

The resolution of the IR microspectroscopy requires special attention. In a regular experiment the IR beam is confined to the sample's area of interest by means of a (usually) rectangular aperture, and the sample is raster-scanned to obtain the spectral map. As with any other microscopy technique, the theoretical resolution in the far field is diffraction-limited, thus, it is dependent on the wavelength of the light. One should expect to achieve a value of a few micrometres; however, resolutions lower than $\sim$20 μm are rarely reported with conventional IR sources (*e.g.*, globar) and point detectors (Fig. 1).[27] This is due to the fact that the flux through the aperture decreases dramatically leading to poor S/N ratios.

Synchrotron IR light sources, which are 100–1000 brighter than thermal IR sources, are one of the ways to overcome this limitation. Another point the experimenter should be aware of is the variation of the resolution across the relevant spectral range: from 2.5 μm at 4000 cm^{-1} to 25 μm at 400 cm^{-1} with 0.5 N.A. objective.

Similar to IR instrumentation, Raman microscopes are realized by coupling Raman spectrometers and research grade optical microscopes. These instruments with excitation wavelengths ranging from near IR to UV are commercially available from a handful of companies. Confocal Raman microscopes allowing for depth scanning are nowadays routinely used in metallurgy, geology, polymer, food and pharmaceutical industries.[28]

Similar to UV-Vis and fluorescence microscopes, the spatial resolution of a Raman microscope is diffraction limited (Fig. 1). When using confocal Raman microscopy one should exercise extreme caution as numerous artefacts may arise from refractive index mismatching, out of focus contributions and improper optical design.[29] Another drawback is an inherently low cross-section of Raman scattering, making the experiments lengthy and prone to ambiguities due to, *e.g.*, laser damage.[30] Several methods to enhance the scattering efficiency have been successfully utilized, among others, resonance Raman[30] and coherent anti-Stokes Raman scattering (CARS).[31] The latter, which is a non-linear pump–probe technique, employs two excitation laser with different wavelength sources to establish the coupling between the ground state and the excited vibrational state.[31] Consequently, the system in the excited state is further excited into a virtual state by a shorter-wavelength laser: upon its relaxation to the ground state an anti-Stokes photon is emitted. CARS is several orders of magnitude more sensitive than normal Raman spectroscopy and possesses an intrinsic sectioning capability of approximately 400 nm in the *x* and *y* directions and approximately 1 μm in the *z* direction, thus enabling the 3-D chemical mapping of small amounts of analytes in confined space with (sub-) micrometre resolution.

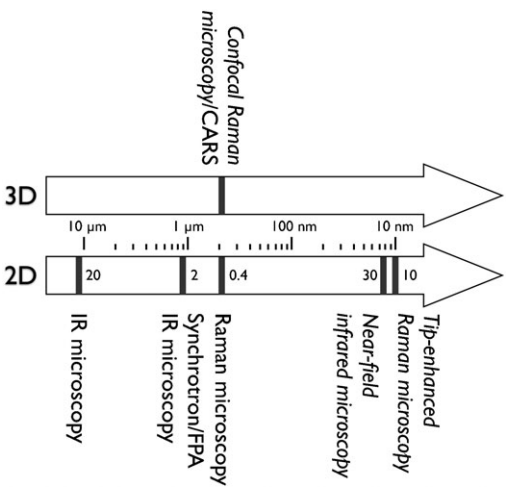

Fig. 1 Overview of the micro-spectroscopic techniques based on vibrational spectroscopy, which are discussed in this tutorial review. The spatial resolution is indicated, while the methods marked in italics have not been as yet applied to problems in heterogeneous catalysis. They are briefly discussed in the Conclusions and outlook section of the article.

To summarize the above section, prior to selecting the method to investigate catalytic system, one ought to consider the limitation of the methods, in terms of (a) resolution, defined by spectral range, intensity of the source and optical configuration (as in confocal Raman microscopes); (b) sensitivity which is a function of the method used, as well as the physics of the underlying processes (as in resonance *vs.* non-resonance Raman scattering); (c) time resolution determined by the sensitivity and the acquisition procedure as in point-by-point *vs.* focal plane detection; and (d) experimental issues, such as experimental cell design and the choice of window material.

Catalyst preparation

The very first application of IR microscopy to a catalyst, namely, a ZSM-5 zeolite, was reported by van Bekkum and co-workers.[32] In this work, the origin of the IR band at 1030 cm^{-1}, often observed in the spectra of micrometre-sized ZSM-5 particles, was unearthed. The spectra of the materials of different morphologies, chemical composition as well as mechanically and thermally activated samples, were compared. The 1030 cm^{-1} band was detected in zeolites with a low Si/Al ratio, which exhibit strongly intergrown structures. On the other hand, the spectra of the individual low-aluminium large ZSM-5 crystal, obtained using IR microscopy, show no distinct bands in the said region. These results led to conclude that the absorption in this spectral region is due to heterogeneity of the zeolite crystallites and impurities on the outer grain surfaces.

IR mapping was utilized for the first time to determine the spatially resolved concentration profile of boron in the partially substituted MFI crystals.[33] Similar to aluminium, trivalent boron isomorphously substitute T-sites in the zeolite framework, resulting in the formation of Brønsted acid sites. These sites, although weaker than their aluminium-based counterparts, make boron–MFI zeolites active in acid-catalyzed reaction, which are not very acidity-demanding. The shift of the 1085 cm^{-1} band was proposed first to be the measure for the degree of T-atom substitution, especially sensitive for low silica zeolites. However, the mapping of the crystal flake with varying thickness has also demonstrated that the position of the band is affected by the length of the optical path in the material. Another indication of the tetrahedral lattice boron presence in the matrix is the Si–O–B vibration at 905 cm^{-1}, which is observed at ambient temperatures. Upon thermal treatment, the water desorption causes transformation of the boron site into a trigonal one, which is characterized by the absorption at 1380 cm^{-1}. Scanning of large B-MFI crystals, as shown in Fig. 2, revealed a uniform distribution of boron across the entire catalyst particle (±0.5 atoms per unit cell). A slight decrease of the intensity at the edges of the crystal was attributed to the deflection of the beam.

Vibrational spectroscopic imaging has proven to be a handy technique to monitor physicochemical processes involved in the preparation of supported catalysts preparation.[34] One of

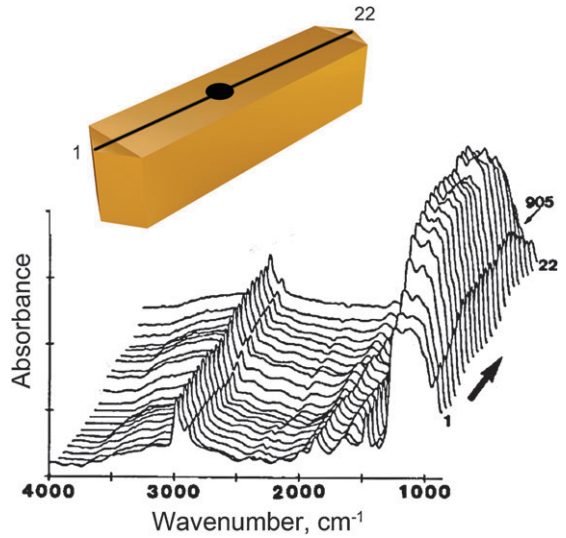

Fig. 2 Stack plot of IR spectra of a large B-MFI zeolite crystal taken along the crystal (dark line) as a function of the beam spot position (adapted from ref. 33, Copyright 1989, with permission from Elsevier).

the common preparation routes of industrial catalysts is the deposition of the active phase on an (inert) micro- or mesoporous support. The size and shape of support bodies are optimized to sustain pressure and temperature operation regime of the reactor. Dimensions of a few millimetres are common. The active component is deposited by impregnation, and the catalyst is dried to remove the solvent and pretreated *via*, *e.g.*, reduction to obtain the desired chemical composition. Strong interaction of the support and the precursor can lead to a non-uniform filling of the support. The temperature and pressure gradients arising during drying and heating may also cause redistribution of the active phase. This can lead to an ineffective use of the catalyst in the process.

The use of Raman micro-spectroscopy for the above application was showcased in the study of molybdenum catalysts supported on Al_2O_3 extrudates (Fig. 3a).[35] The MoS_2 are employed in hydrotreating processes in which sulfur, nitrogen and metals are removed from oil fractions. The activity of the resulting catalyst, which also contains promotors, such as Ni or Co, is strongly dependent on the MoS_x phase formed. As a consequence, the impregnation step is of crucial importance. Fig. 3b and c shows the distribution of the Mo precursor complex in the support pellet at different times after impregnation. One can see that, even though the capillary forces in the pore system make the water filling almost instantaneous, it takes hours for the system to equilibrate due to the interaction between the metal complexes in solution and the surface of the support. The Mo complexes formed within the extrudate pores due to local pH variation and the chemical interaction between the precursor and the support could be speciated.[36]

After impregnation, the Mo/Al_2O_3 catalysts are dried and calcined to obtain a MoO_3 which consequently undergoes sulfidation. When the pH of the impregnating solution was not adjusted, the drying resulted in an egg-shell distribution, that is, an enrichment of the outer layer of the pellet. When the capacity of the support was exceeded, a bulk MoO_3 phase was formed during calcination in the near-surface regions. Adding

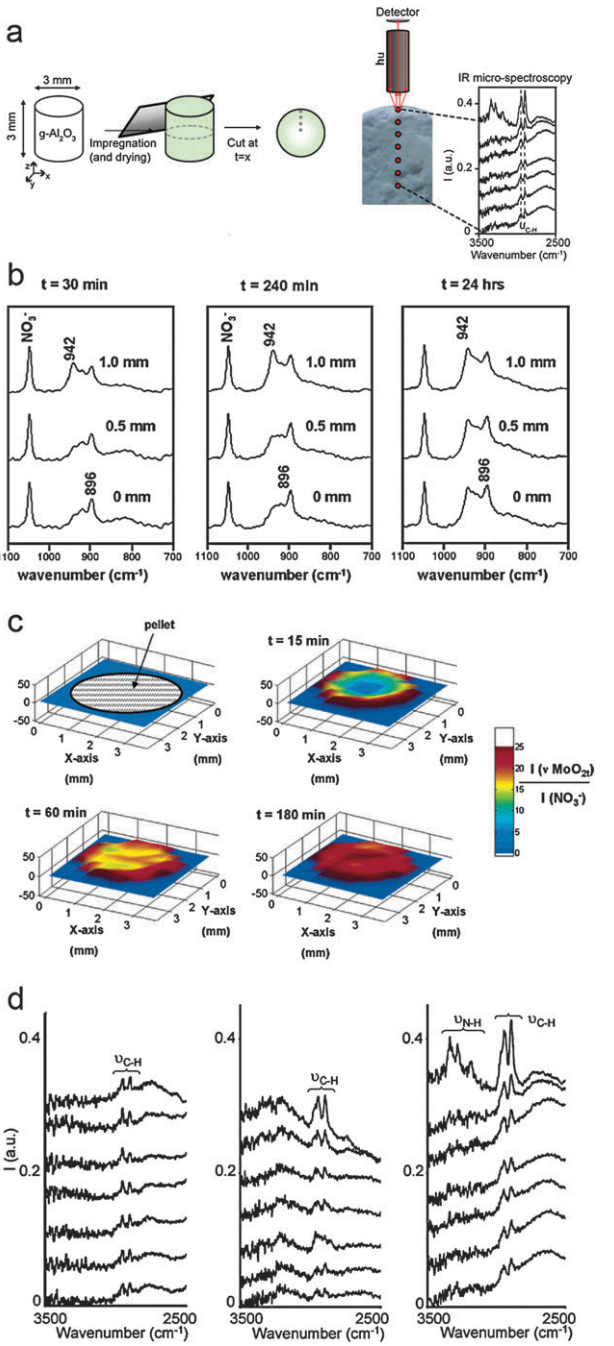

Fig. 3 (a) Experimental approach when an invasive technique is used to characterize impregnated or dried pellets and the example of the dissected pellet together with the spatially resolved spectra; (b) Raman spectra of catalyst support bodies impregnated with ammonium heptamolybdate solutions. The Raman laser was focused at 0, 0.5, and 1.0 mm from the centre; (c) 2-D Raman spectroscopy profiles illustrating the spatial distribution of the molybdenum anions in 3 mm-sized Al_2O_3 pellets taken 15, 60, and 180 min after impregnation with a Mo–citrate solution; (d) IR spectra (spatial resolution of 200 μm) collected from the edge to the centre (top to bottom) of dried bisected $Ni/\gamma\text{-}Al_2O_3$ pellets for the initial impregnating solution with Ni/ethylene diamine ratio equal to 1 : 1 (left), 1 : 2 (centre), and 1 : 3 (right) (reprinted with permission from ref. 35 and 37, Copyright 2004 and 2008 American Chemical Society).

citrate to the impregnating solution was found to improve the catalyst dispersion; this was also found to correlate with hydrodesulfurisation activity.[36] It was also shown that when the cobalt (promotor) salt is added to impregnating molybdate solution, a binding between the cobalt ions and various molybdate ions assists in simultaneous transport of the two components in the support body.[38] We should emphasize that the phenomena described above would be overlooked with powdered samples and could only be deduced using a spatially resolved spectroscopic methodology.

As the citrate example above shows, adding the complexing and chelating agents at the impregnation step alters the strength of the interaction between the metal ions and the support surface. In another example, ethylenediamine was used in the preparation of the hydrogenation Ni-based catalysts.[37] Here, the concentration profiles of the Ni complexes in the pellets after impregnation were determined with UV-Vis micro-spectroscopy. IR micro-spectroscopy was used to map the concentration of the ligand after drying procedure and the results are summarized in Fig. 3d.

One should be aware that the proposed imaging scheme is an invasive one: the support body is cut at various stages of the preparation process. This dissection of the pellet can disturb the distribution of the solvated active phase, due to solvent evaporation through the new interface. To exclude the uncertainties, the cross-reference with non-invasive methods is required to validate the findings as was done using *e.g.* magnetic resonance imaging (MRI) and tomographic diffraction imaging (TEDDI) on extrudates bodies.[39–42]

High-throughput studies

Another potent application of IR microscopy is in high-throughput studies.[43] Multi-reactor manifolds are routinely used for parallel catalyst characterization. However, by and large the only variable available for process control and optimization is the sequential gas analysis at the outlet of the system, by means of the gas-chromatographer or mass spectrometer, which does not allow for a high degree of parallelization.

A first promising example in this direction was the application of IR thermography,[44] which albeit high spatial and temporal resolution suffers from lack of chemical information. These methods could have been upgraded to real spectral imaging with the arrival of focal plane array (FPA) detectors, which comprise a grid of small elements, usually of mercury–cadmium–telluride (MCT) type. The first transmission cell was developed for the analysis of the gas products and successfully used for the screening of γ-Al_2O_3-supported Pt and Pd catalysts with different metal concentration in propene oxidation.[45] However, the transmission geometry limits the number of channels that can be addressed in parallel to the maximum of 16. To overcome this constraint, a reflection cell with 49 channels has been developed (Fig. 4).[43] The radiation is fed into the cell through the IR-transparent CaF_2 window, travels along the capillary and is reflected by a gold mirror in the bottom back to the detector. The system was benchmarked with the pentane hydroisomerisation reaction on Pt/mordenite zeolites. This reaction, relevant in the petroleum industry, is on one hand simple with little formation of by-products, and on the other, very demanding due to the little differences in the spectra of the reagent and products. Careful calibration and spectral deconvolution have permitted the differentiation of the two components of the gas mixture with a relative error of $\sim$10%, which makes the system suitable for pre-screening of catalysts.

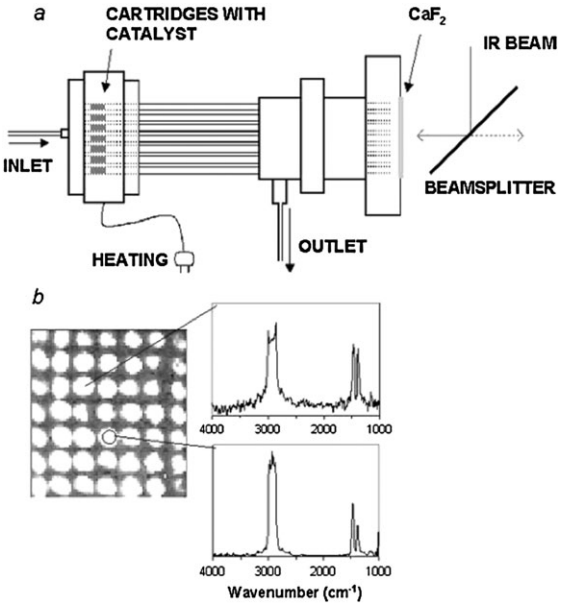

Fig. 4 (a) Schematic view of the 49-fold reactor and the analysis cell for IR measurements in reflection mode. The stainless steel capillary inner diameter is $\sim$4 mm; (b) the image of the capillary bundle on the FPA detector. Right top, IR spectrum of one pixel; right bottom, IR spectrum combined from 30 pixels (reprinted with permission from ref. 43, Copyright 2004 American Chemical Society).

Not only gas phase reaction products could be analyzed by high-throughput IR imaging. Characterization of acidic properties in a series of zeolites using pyridine as a probe molecule has been reported by Busch *et al.*[46] A vacuum-tight transmission sandwich cell, comprising two CaF_2 windows, could accommodate up to eight samples for simultaneous imaging. A heating element inside the chamber allowed for a pre-treatment of the samples under identical conditions. With this design, the degree of parallelization can be easily increased as well as the temperature and pressure ranges. The quality of the data obtained with the cell is not inferior to the conventional analysis, and is not limited to pyridine adsorption experiments.

Adsorbates: orientation and diffusion

Adsorbate adsorption and diffusion in molecular sieves is the field in which IR imaging has unveiled its full potential, especially, when combined with other techniques, such as interference microscopy. The first study of this kind has been reported by Schüth.[47] The silicalite-1 crystals were loaded with *p*-xylene and the IR spectra with polarized radiation were taken from the individual crystals to reveal the structure of the adsorbate in zeolites. When the light polarization was aligned perpendicular to the crystal long axis, strong IR bands appeared at 2923, 2867 and 1518 cm^{-1}; while at parallel

orientation the IR bands vanished. Analysis of the vibration modes for *p*-xylene shows that the transition moment associated with these vibration modes changes in the *z* direction that is along the long axis of the molecule. From these results it could be inferred that the adsorbate molecules align perpendicular to the long axis of the crystal. Edges of the crystals, however, showed different behaviour: spectra were found to be polarization independent (Fig. 5b). The intergrowth architecture of the MFI-type crystals has unfortunately not been elucidated at that time; with today's knowledge on the orientation of the channel system in different regions of the crystal[48] the results can be straightforwardly rationalized. In the centre of the silicalite crystal the straight channels accommodating *p*-xylene molecule are directed perpendicularly to the crystal long axis. At the edges, due to the twinning, the straight channels run along the *b*-direction (Fig. 5), coinciding with the incidence direction of incoming IR radiation; therefore, spectra are not influenced by changes in polarization. Similarly to MFI, *p*-xylene adsorbed in aluminophosphate SAPO-5 crystals aligns along the uni-dimensional pores of this molecular sieve.[49]

An orientation of probe molecules in the channels of metal-substituted microporous aluminophosphates and their interaction with acid sites have been also investigated using single micron-sized AlPO-5 crystals. Using ammonia and pyridine as acidity probes, Brønsted acid sites have been observed for the first time in beryllium- and magnesium-substituted AlPO-5 and SAPO-5.[50] IR bands characteristic of protonated ammonia appeared in the spectra, whereas in the case of non-substituted

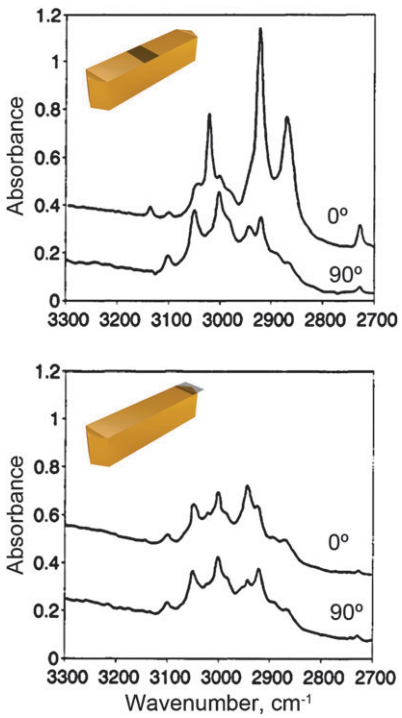

Fig. 5 Spatially resolved polarized spectra of a *p*-xylene loaded silicalite I. $\theta = 0°$ corresponds to polarization perpendicular to the crystal's *c*-axis. Crystal orientated with (010) parallel to beam axis. Top: middle of crystal. Bottom: end of crystal (reprinted with permission from ref. 47, Copyright 1992 American Chemical Society).

$AlPO_4$-5 Lewis acid sites were detected. Using benzene for probing Brønsted acidity in SAPO-5 revealed a preferred orientation of the molecules in the pores.[51] However, the alignment imposed by the channel system on this relatively symmetric molecule is not very strict. The same observation has been made for acetonitrile. In the case of pyridine, variations in orientations of the molecules were detected for different adsorption sites and their acid strengths. Both Lewis and Brønsted in SAPO-5 force pyridine and pyridinium ion molecules to align parallel to the pore vector, whereas in the case of GaAPO-5 the preferred orientation is orthogonal to the direction of the channel. Physisorbed pyridine moiety is ordered in the same manner.

Howe *et al.* have used polarized IR microscopy to investigate template interaction in $AlPO_4$-5 and SAPO-5 crystals.[52] The triethylamine molecules, which are fully protonated and strongly hydrogen-bound to the framework in the as-synthesized material, lose water upon thermal treatment, yielding a neutral species. The template in both protonated and non-protonated forms was found to align with the C_3 symmetry axis parallel to the pore direction.

IR microscopy has also proven to be advantageous in investigating dynamic adsorption processes. In a typical experiment the pre-treated zeolite crystal is exposed to the pressure of the adsorbate; subsequently, a concentration profile is mapped in time. Modelling of the temporal changes in intracrystalline concentration of the adsorbate allows elucidating diffusion parameters. As mentioned above, aperture based IR microscopy suffers from insufficient spatial resolution. Therefore, it is often used in conjunction with interference microscopy. Comparison of the profiles obtained by both methods is key to quantify the interference signal. In such a way, intracrystalline diffusion boundaries and, consequently, the intergrowth structure of the crystal could be visualized (Fig. 6).[53]

In certain cases the imaging of the entire zeolite particle could bring sufficient information about the diffusion process. In this manner, adsorption of isobutane on MFI-type crystals has been studied.[54] The crystals were modified by silylation in order to produce external surface barriers of different strength. The strength of the barrier was modified by using trimethyl-, triethyl- and tripropylchlorosilane. The uptake rates were found to decrease with the increase in the bulkiness of the alkyl groups due to the partial blocking of the pore mouth.

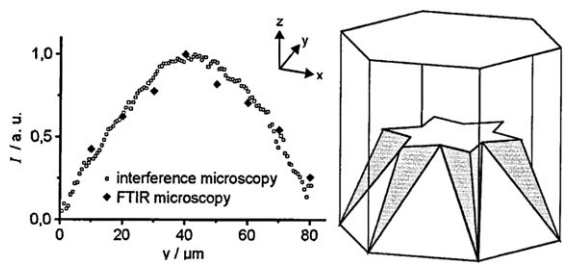

Fig. 6 (a) Mean concentration integrals of methanol adsorbed on CrAPO-5 crystals recorded by FT-IR and interference microscopy. (b) Suggested internal structure of CrAPO-5 crystals based on these measurements (adapted with permission from ref. 53, Copyright 2002 American Chemical Society).

In the same manner, a molecular uptake of alkanes in the metal–organic framework (MOF) CuBTC crystals was investigated.[55] It should be noticed though that in the present case the method could not provide the microscopic-scale information on the nature of the surface diffusion barriers.

The appearance of FPA detector technology allowed to partially overcoming the spatial resolution shortcoming, unveiling truly microscopic capabilities of the technique. In the first demonstration of the method, the nature of the surface barriers in MOF Zn(tbip) crystals has been explored.[56] To evaluate the role of the diffusion-hindering defects, arising during crystallization process, such as crystal overgrowths on the external surface, crystals of different history were investigated (Fig. 7a and b). Some crystals were broken prior to the measurements to compare the properties of the ''old'' (created in the course of preparation or due to the material aging) and ''new'' surfaces. The concentration profiles of propane in the broken Zn(tbip) crystal (Fig. 7d) appear asymmetric, clearly showing the differences in the surface permeabilities between the ''new'' and ''old'' surfaces. Symmetry is re-established in crystals with two freshly broken surfaces crystal (Fig. 7c). In another MOF material, ZIF-8, an interesting phenomenon, namely the enhancement of the mass transfer by the flux of molecules in an opposite direction has been discovered.[57]

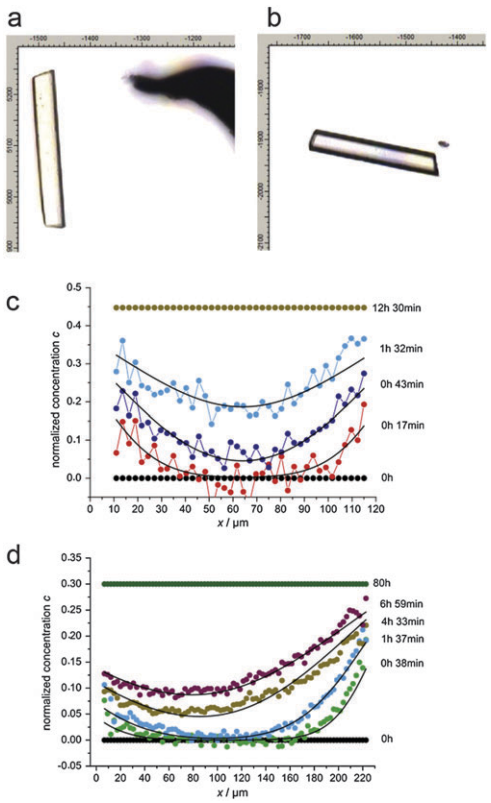

Fig. 7 MOF Zn(tbip) crystal (tbip, 5-*tert*-butylisophthalate) with a total length of about 300 μm, before (a) and after (b) a piece of about 20–30 μm has been broken off, by using the tip of a needle; (c) evolution of the concentration profiles of propane in the intact MOF Zn(tbip) shown in (a) along the longitudinal crystal axis during molecular uptake; (d) the same as (c) for the crystal with one freshly created surface shown in (b). The concentration profiles are normalized with respect to a saturation loading of 1 molecule per pore segment. Full lines show the results of numerical solutions of Fick's second law providing the best fit to the measured concentration profiles (reprinted from ref. 56, Copyright 2010, with permission from Elsevier).

Reactivity and *in situ* studies

With the development of IR imaging instrumentation it was only a matter of time that the method has been applied to follow real chemical reactions. The first attempt, which merited the prefix *in situ*, concerned the process of thermal decomposition of the template in MFI-type materials.[58] These organic compounds are added to zeolite crystallization solution to act as structure-directing agents in order to sustain the channel architecture of micro- and mesoporous materials. After preparation, the template has to be removed to vacate the pores for adsorbates and/or reactants, usually by high temperature treatment. In the present case, the chemical transformations of the tetrapropylamine template in large individual MFI crystals were studied upon calcination up to 773 K using IR microscopy.

As-synthesized zeolites at ambient temperatures showed broad lattice bands as well as the vibrations identical to the IR spectra of tetrapropylammonium ions in solution (Fig. 8). The presence of asymmetric CH deformation bands similar to those in the solid state indicated relatively low mobility of the template molecules. Upon heating the ratio of the band intensities corresponding to CH_3 and CH_2 groups decreased, pointing out at the elongation of the hydrocarbon chains due to partial oligomerization. Mobility of the ions increases in the temperature range up to 613 K as evidenced by the CH deformation spectra region. Above 633 K the CH stretching vibrations intensified with remarkable differences between samples with varying Al concentration. Further on, the template molecules decompose *via* Hoffman elimination, *i.e.*, removal of the alkyl chain in the form of alkene, and formation of tripropyl amine in Al-deficient zeolite samples or tripropyl ammonium cation in Al-enriched zeolite samples due to the interaction with acid sites. Further decomposition follows the same route leading to the formation of alkenes and ammonia.

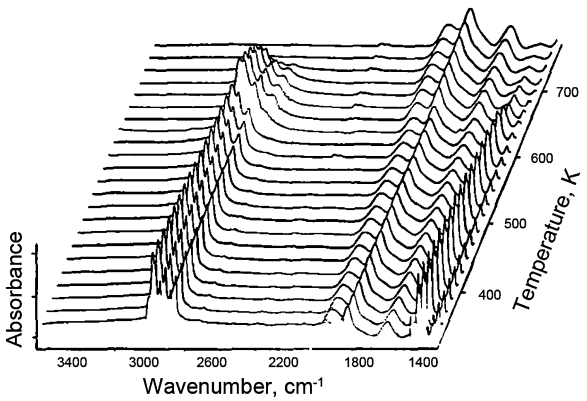

Fig. 8 *In situ* IR spectra of an individual ZSM-5 crystal recorded during the thermal decomposition of the tetrapropylammonium template (adapted from ref. 58, Copyright 1991, with permission from Elsevier).

Even though microscopy has been utilized in the investigations discussed above, only one spot as large as 30 μm on the crystal had been measured. The mapping of the crystal in the course of template decomposition could have been revealed the spatial distribution of the template molecules; however, better spatial resolution is required. This can be achieved using synchrotron IR light, as the high photon flux of this source makes it possible to decrease the aperture down to a few micrometres with only moderately sacrificing the sensitivity. This approach is exemplified in a recent study on the reactivity of large ZSM-5 crystals.[59] The oligomerization of styrene derivatives initiated by Brønsted acid zeolite sites has been chosen as probe reaction for catalytic activity. This ZSM-5/styrene system was investigated using UV-Vis and fluorescence micro-spectroscopy,[17,19,60] and the styrene oligomerization reaction has been found to be a very sensitive probe for zeolite acidic properties and porosity as well as electronic properties of the substituted styrene. The recent combined experimental and theoretical study allowed to directly connect the geometric parameters of the zeolite voids and the reaction pathways and selectivity.[61]

The optical microscopy study provided striking evidence towards the direct link between the spatial differences of the crystal microporous structure and the spatial distribution of the reaction products. The way the pore system of the MFI structure consisting of the straight channels intersected with zigzag channels is interconnected with the outer surface of the zeolites defines the diffusion of the reactant molecules to the active sites. That in turn resulted in the formation of dimeric and trimeric oligomers at different regions on the crystal, which was found to correlate with the orientation of porous systems in the crystal segments.[62] The optically active species observable by optical and fluorescence microscopies[17,19] were assumed to be carbocationic oligomers of different lengths stabilized on acid sites; however their exact chemical nature devised from the general chemical considerations was somewhat ambiguous.

IR micro-spectroscopy helped to shed light into the chemical structure of the intermediates which served as markers for the zeolite catalytic activity and the results are summarized in Fig. 9. In a first experiment, the ZSM-5 crystals were exposed to 4-fluorostyrene, heated to 373 K and the IR spectra from the 5 μm × 5 μm region in the centre of the crystal were taken (Fig. 9a). Two sharp features at 1534 cm^{-1} and 1510 cm^{-1} could be discerned in the spectrum. Comparison of the spectra with that of 4-fluorostyrene (Fig. 9b) shows that the band at 1510 cm^{-1} was due to the reactant. When the spectra were taken during the reaction (Fig. 9c) in the *in situ* cell, the intensity of the latter band dropped, while the IR band at around 1534 cm^{-1} increased. This behaviour clearly indicates that the origin of the latter IR absorption is the species formed during the reaction, *i.e.*, styrene oligomers.

Synchrotron IR radiation is intrinsically polarized and this property can be utilized to investigate oriented systems, such as molecules in zeolite channels. In the present case the assignment of the 1534 cm^{-1} band has been supported by measuring polarization dependence of the band intensity. When the light was polarized along the direction of the straight channels, which accommodate long oligomer molecules, the intensity of the band was significantly higher than the one taken at perpendicular polarization (Fig. 9d), in

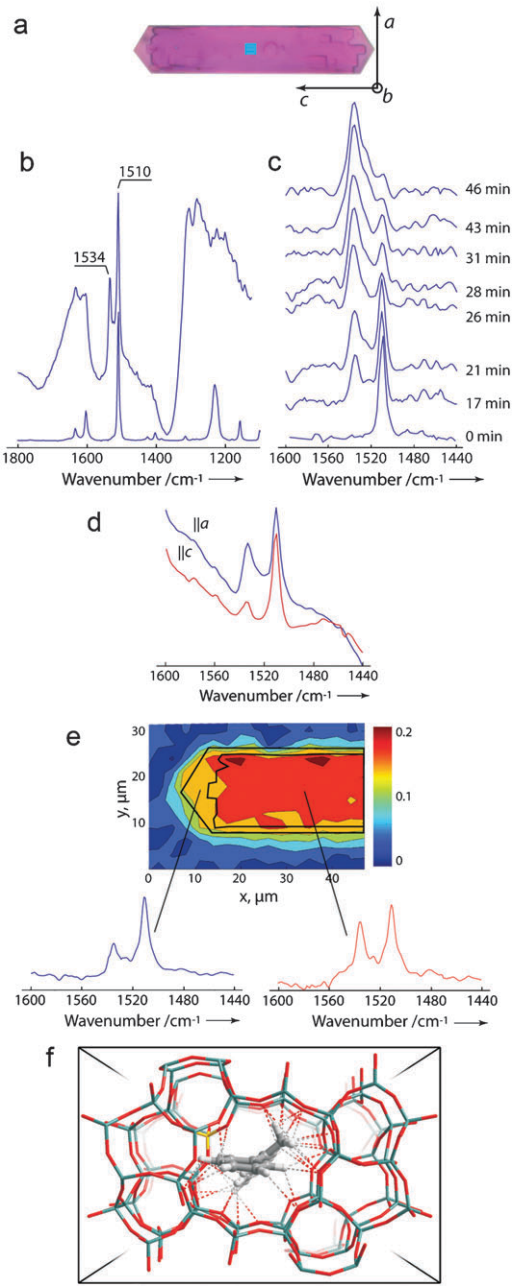

Fig. 9 (a) Optical microphotograph of the H-ZSM-5 crystal after reaction with 4-fluorostyrene with the square probed area marked; (b) IR spectrum of an individual H-ZSM-5 crystal contacted with 4-fluorostyrene (top) and the IR spectrum of liquid 4-fluorostyrene (bottom); (c) 1440–1600 cm^{-1} region of the IR spectra taken *in situ* during the 4-fluorostyrene oligomerization reaction. The spectra are background corrected; (d) *in situ* IR spectra taken with two different light polarizations; (e) intensity of the IR band at 1534 cm^{-1} mapped over the crystal after reaction and the IR spectra taken from the edge and the body of the crystal, demonstrating differences in the intensity ratio of the bands; (f) optimized geometry of linear conjugated carbocation formed during styrene oligomerization in the straight channel of H-ZSM-5, which is responsible for the IR band (from ref. 63 and 64, Copyright Wiley-VCH Verlag GmbH&Co. KGaA, reproduced with permission).

agreement with the optical absorption measurements.[17] Comparison of the experimental data with the spectra calculated for relevant carbocationic structures confirmed the assignment.

With the spatial resolution provided by synchrotron-based IR micro-spectroscopy the spatial distribution of the reaction products can be established. The zeolite particle after the reaction was raster-scanned and the spatial map of the 1534 cm^{-1} band is shown in Fig. 9e. The spatially resolved IR spectra are in line with the UV-Vis and confocal fluorescence data with lower intensity of the dimer band at the edges as compared to the body of the crystal.

It should be noticed that a rigorous theoretical analysis of IR spectra should be carried out in order to rationalize the polarization dependence phenomenon in molecules occluded in zeolite matrices.[64] DFT calculations of the IR spectra of the styrene dimeric carbocation trapped in the zeolite pore (Fig. 9f) allow singling out the vibration mode responsible for the strong IR absorption at 1534 cm^{-1}. The direction of the dipole moment change associated with the molecular movement was found to be collinear with the long axis of the molecule and, in turn with the direction of the straight pore. Interestingly, carbocationic intermediates could only be detected in large ZSM-5 crystals and not in zeolite powders, due to mediated diffusion rates of the reactants to the reaction sites that prevent polymerization and allow for stabilization of otherwise evasive reaction intermediates. This makes the combination of IR microscopy and the usage of well ordered zeolite particles a superior tool in elucidating catalytic reaction mechanisms.

One can notice from the above discussion that IR micro-spectroscopy is capable of mapping reaction products in an individual catalyst particle with micrometre spatial resolution. The final reaction product profile is the result of a combination of the spatial inhomogenities in reactivity and initial reagent distribution. The latter can be directly determined with Raman micro-spectroscopy if the reagent exhibits strong features in the spectrum.

For this purpose, the catalytic thiophene conversion on individual ZSM-5 crystals was chosen to showcase the CARS imaging capabilities.[65] Thiophene was contacted with the zeolite at room temperature and after equilibration its distribution over the particle has been visualized by 3-D raster scanning. The resulting spectra were analyzed using the maximum entropy method to establish quantitative Raman responses. The Raman band at 3115 cm^{-1} assigned to =C–H stretching modes of intact thiophene molecules (Fig. 10a) was used as a measure for the local thiophene concentration. The reconstructions of the 3-D concentration profiles are shown in Fig. 10b. One can see that thiophene is concentrated in the bulk of the crystal and an hourglass pattern can be discerned, illustrating the effect of diffusion barriers at the crystal subunits boundaries.

Unfortunately, the attempts to follow the catalytic thiophene conversion with the CARS technique have failed due to strong fluorescence background, which obscures the Raman signal. Thus, IR micro-spectroscopy had to be employed to reveal the reaction pathways. Upon heating, several new IR bands arise in the thiophene ring stretching

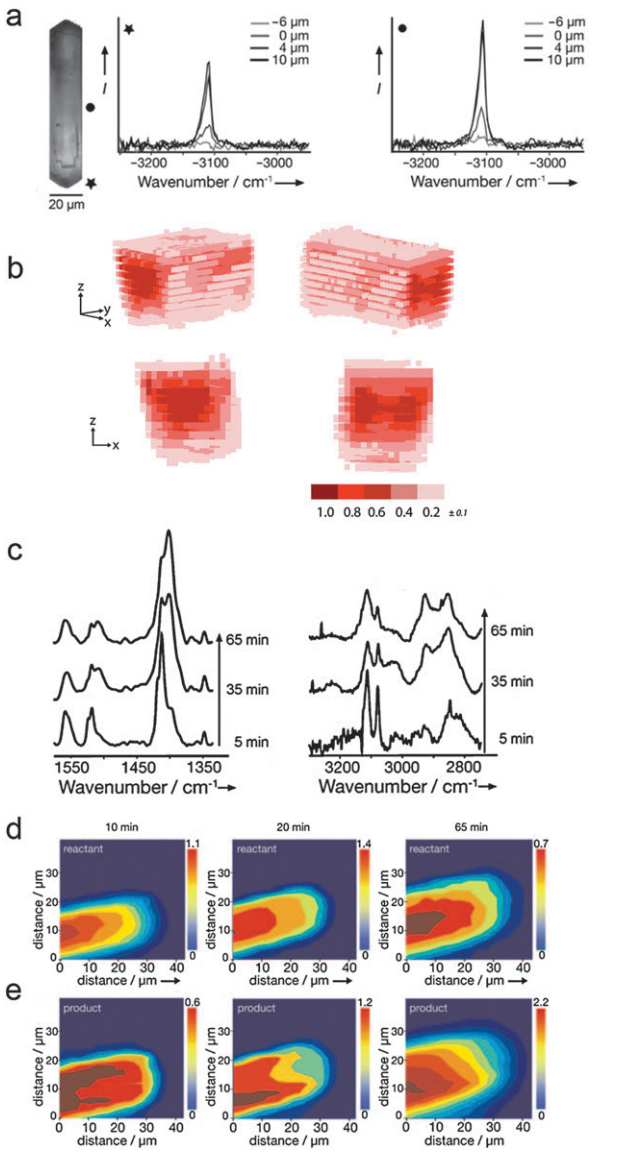

Fig. 10 (a) Nonlinear Raman responses measured at the edge (asterisk) and the centre (full circle) of the crystal for different depths; (b) 3-D nonlinear Raman response images. 2-Chlorothiophene concentration based on 3115 cm^{-1} band intensity for the lower (left) and upper (right) edges of the crystal shown in (a); (c) IR spectra of the ring stretching region (left) and C–H stretching (right) measured in the centre of the crystal after 5, 35, and 65 min of reaction; (d) 2-D IR intensity maps of a 2-chlorothiophene/H-ZSM-5 crystal after (a) 10, (b) 20, and (c) 65 min of reaction for the 1412 cm^{-1} reactant band; and (e) the same as (d) for the 1401 cm^{-1} product band (from ref. 65, Copyright Wiley-VCH Verlag GmbH & Co. KGaA, reproduced with permission).

vibrations (Fig. 10c). Those IR bands appeared to be strongly polarization dependent, pointing out at their origins as elongated thiophene oligomerization products, aligned in the zeolite ZSM-5 straight channels. IR spectral features indicate that both reaction pathways with ring opening and thiophene condensation with rings intact are active in the present system. The IR intensity maps (Fig. 10d and e) were in excellent correlation with those obtained by CARS.

We would like to emphasize again the wealth of *in situ* spectroscopy data that could be obtained using vibrational methods, due to their chemical insight, which can be only indirectly attained by other methods. On the other hand, both examples of catalytic styrene and thiophene conversion demonstrate the importance of combining IR and Raman micro-spectroscopy with other methods, which feature comparable spatial resolution and deliver information of different aspects of the chemical process under investigation. In this respect, it has been recently shown for the catalytic thiophene conversion that the combination of X-ray, IR, Raman, confocal fluorescence and UV-Vis micro-spectroscopy on the same individual ZSM-5 zeolite crystals can deliver a wealth of information regarding the spatial heterogeneities, molecular diffusion barriers and chemical reactivity of individual catalyst particles.[66]

Conclusions and outlook

The above overview of literature data clearly demonstrates the advantages vibrational micro-spectroscopic methods have to offer in the field of heterogeneous catalysis. Beyond the existing capabilities, there are a number of developments, which, if fully realized, can enable the researcher with even greater possibilities.

As discussed above, the two most effective ways to circumvent the inherently low spatial resolution of IR micro-spectroscopy are using high-brilliance synchrotron light and area detectors, such as FPA. Evidently, the marriage of the two would be more than welcome, boosting both simultaneously the resolution and sensitivity. Unfortunately, the synchrotron light is collimated into a relatively narrow beam, which is unable to illuminate the entire detector plane. Intricate and somewhat cumbersome measures are taken to spread the beam over the detector by means of individually controlled mirrors, which are used to split and refocus the light. It remains to be seen whether the robust solution is possible. Moreover, at the majority of the IR synchrotron beamlines, bending magnets are used to deflect the electron beam; therefore the emanating light is linearly polarized. Circularly polarized light could be generated with indulators, which are routinely used for other spectral ranges, *e.g.*, X-rays. The potential of circularly polarized IR radiation for investigating chiral porous materials structures and chiral catalytic reactions, as well as for advanced methods, *e.g.*, sum-frequency generation spectroscopy[67] have not been explored as yet. In addition, synchrotron-based IR beamlines provide a unique opportunity for implementing time-resolved IR spectroscopy. Synchrotrons operate with electrons traveling in bunches around the storage ring, and the radiation is emitted when the electron bunch is forced to change its trajectory in a bending magnet or indulator. This creates a train of light pulses with a nanosecond temporal separation, which can be used for time-resolved measurements and pump–probe experiments.

Besides synchrotrons, another tremendously powerful source of radiation is the free-electron laser (FEL). In this device, a pre-accelerated bunch of electrons passes through a periodic magnetic field, creating a coherent light beam. The radiation emitted from the FEL is monochromatic and its wavelength can be adjusted by varying magnetic field strength and/of electron beam energy. With a monochromatic IR radiation, confocal imaging that is the depth profiling in addition to the lateral scanning can be in principle realized, similar to the existing confocal fluorescence and Raman techniques.

As to Raman spectroscopy, one of the most promising directions is the combination of this method with scanning probe microscopy (SPM). The latter can detect single molecule transformations, as in the example of direct observation of oxidation of the manganese ion coordinated by porphyrine macrocycle with molecular oxygen.[68] If the topographic measurements with sub-nanometre accuracy by SPM could be integrated with spectroscopic detection, capable of delivering direct chemical information, a breakthrough tool would emerge. Tip-enhanced Raman spectroscopy (TERS) takes advantage of the effect of local enhancement of the electromagnetic fields in the vicinity (at 1–10 nm distance) of the rough noble metal surface of metal nanoparticle. This enhancement brings about a tremendous boost in the Raman scattering cross-section, up to several orders of magnitude. In TERS, the nanoparticle is mounted on the SPM tip (or, alternatively, the entire tip is metal coated), and the surface is scanned, accompanied by laser excitation.[69] In this way, the Raman-active molecule can be localized and identified. Single molecule detection by TERS has been reported.[70] It appears that it is just a matter of overcoming a number of technical hurdles to see the technique applied for studying catalytic systems.

Another approach to boost the spatial resolution beyond the diffraction-limited values is by employing the so called near-field geometry. In this method, either the sub-wavelength-sized excitation source or the detector, *e.g.*, tapered optical fiber is positioned very closely (within a fraction of the wavelength) to the specimen surface. In the first successful application of the near-field Raman scattering[71] to benzene hydrogenation to cyclohexane on model Pd catalysts structural changes of the adsorbates on the activated surface and the possible intermediates were detected. Recently, reports on the implementation of near-field IR microscopy have also appeared.[72] Possibilities of both aperture-based and aperture-less operation modes should therefore be explored.

Acknowledgements

We thank the Dutch National Science Foundation (NWO-CW VICI, VENI and TOP Grant) and Research School Combination Catalysis (NRSC-C) for financial support.

Notes and references

1 R. A. van Santen and M. Neurock, *Molecular Heterogeneous Catalysis: A Conceptual and Computational Approach*, Wiley-VCH, Weinheim, 2005.
2 R. P. Eischens, W. A. Plisken and S. A. Francis, *J. Chem. Phys.*, 1954, **24**, 1786.
3 R. P. Eischens and W. A. Pliskin, in *Advances in Catalysis and Related Subjects*, ed. D. D. Eley, W. G. Frankenburg and V. I. Komarewsky, Academic Press, New York, 1958, p. 2.
4 *In-situ Spectroscopy in Heterogeneous Catalysis*, ed. J. F. Haw, Wiley-VCH, Weinheim, 2002.

5 *In-situ Spectroscopy of Catalysts*, ed. B. M. Weckhuysen, American Scientific Publishers, Stevenson Ranch, 2004.
6 M. A. Banares and G. Mestl, *Adv. Catal.*, 2009, **52**, 43.
7 F. C. Jentoft, *Adv. Catal.*, 2009, **52**, 129.
8 C. Lamberti, E. Groppo, G. Spoto, S. Bordiga and A. Zecchina, *Adv. Catal.*, 2007, **51**, 1.
9 A. Bruckner, *Adv. Catal.*, 2007, **51**, 265.
10 L. F. Gladden, M. D. Mantle and A. J. Sederman, *Adv. Catal.*, 2006, **50**, 1.
11 S. R. Bare and T. Ressler, *Adv. Catal.*, 2009, **52**, 339.
12 A. Knop-Gerricke, E. Kleimenov, M. Havecker, R. Blume, D. Teschner, S. Zafeiratos, R. Schlogl, I. V. Bukhtiyarov, V. V. Kaichev, I. P. Prosvirin, A. I. Nizovksii, H. Bluhm, A. Barinov, P. Dudin and M. Kiskinova, *Adv. Catal.*, 2009, **52**, 213.
13 B. M. Weckhuysen, *Angew. Chem., Int. Ed.*, 2009, **48**, 4910.
14 G. A. Somorjai and Y. Li, *Introduction to Surface Chemistry and Catalysis*, Wiley, New York, 2nd edn, 2010; G. Ertl, *Reactions at Solid Surfaces*, Wiley, New York, 2009.
15 B. M. Weckhuysen, *Chem. Commun.*, 2002, 97.
16 B. M. Weckhuysen, *Phys. Chem. Chem. Phys.*, 2003, **5**, 4351.
17 M. H. F. Kox, E. Stavitski and B. M. Weckhuysen, *Angew. Chem., Int. Ed.*, 2007, **46**, 3652.
18 M. B. J. Roeffaers, B. F. Sels, H. Uji-i, F. C. De Schryver, P. A. Jacobs, D. E. De Vos and J. Hofkens, *Nature*, 2006, **439**, 572; M. B. J. Roeffaers, G. De Cremer, H. Uji-i, B. Muls, B. F. Sels, P. A. Jacobs, F. C. De Schryver, D. E. De Vos and J. Hofkens, *Proc. Natl. Acad. Sci. U. S. A.*, 2007, **104**, 12603.
19 E. Stavitski, M. H. F. Kox and B. M. Weckhuysen, *Chem.–Eur. J.*, 2007, **13**, 7057.
20 E. de Smit, I. Swart, J. F. Creemer, G. H. Hoveling, M. K. Gilles, T. Tyliszczak, P. J. Kooyman, H. W. Zandbergen, C. Morin, B. M. Weckhuysen and F. M. F. de Groot, *Nature*, 2008, **456**, 222.
21 E. de Smit, I. Swart, J. F. Creemer, C. Karunakaran, D. Bertwistle, H. W. Zandbergen, F. M. F. de Groot and B. M. Weckhuysen, *Angew. Chem., Int. Ed.*, 2009, **48**, 3632.
22 F. M. F. de Groot, E. de Smit, M. M. van Schooneveld, L. R. Aramburo and B. M. Weckhuysen, *ChemPhysChem*, 2010, **11**, 951.
23 J.-D. Grunwaldt, S. Hannemann, C. G. Schroer and A. Baiker, *J. Phys. Chem. B*, 2006, **110**, 8674.
24 L. F. Gladden, *Top. Catal.*, 2003, **24**, 19.
25 I. V. Koptyug, A. A. Lysova, R. Z. Sagdeev, V. A. Kirillov, A. V. Kulikov and V. N. Parmon, *Catal. Today*, 2005, **105**, 464.
26 G. L. Carr, *Rev. Sci. Instrum.*, 2001, **72**, 1613.
27 L. M. Miller and R. J. Smith, *Vib. Spectrosc.*, 2005, **38**, 237.
28 *Infrared and Raman Spectroscopic Imaging*, ed. R. Salzer and H. W. Siesler, Wiley-VCH, Weinheim, 2009.
29 N. J. Everall, *Appl. Spectrosc.*, 2009, **63**, 245A.
30 E. Smith and G. Dent, *Modern Raman Spectroscopy: A Practical Approach*, Wiley, Chichester, 2004.
31 J. X. Cheng and X. S. Xie, *J. Phys. Chem. B*, 2004, **108**, 827.
32 R. A. le Fèbre, J. C. Jansen and H. van Bekkum, *Zeolites*, 1987, **7**, 471.
33 J. C. Jansen, R. de Ruiter, E. Biron and H. Van Bekkum, in *Zeolites; Facts, Figures, Future*, ed. P. A. Jacobs and R. A. van Santen, Elsevier, Amsterdam, 1989.
34 L. Espinosa-Alonso, A. M. Beale and B. M. Weckhuysen, *Acc. Chem. Res.*, 2010, **43**, 1279.
35 J. A. Bergwerff, T. Visser, B. R. G. Leliveld, B. D. Rossenaar, K. P. de Jong and B. M. Weckhuysen, *J. Am. Chem. Soc.*, 2004, **126**, 14548.
36 J. A. Bergwerff, M. Jansen, B. G. Leliveld, T. Visser, K. P. de Jong and B. M. Weckhuysen, *J. Catal.*, 2006, **243**, 292.
37 L. Espinosa-Alonso, K. P. de Jong and B. M. Weckhuysen, *J. Phys. Chem. C*, 2008, **112**, 7201.
38 J. A. Bergwerff, T. Visser and B. M. Weckhuysen, *Catal. Today*, 2008, **130**, 117.
39 A. A. Lysova, I. V. Koptyug, R. Z. Sagdeev, V. N. Parmon, J. A. Bergwerff and B. M. Weckhuysen, *J. Am. Chem. Soc.*, 2005, **127**, 11916.
40 A. M. Beale, S. D. M. Jacques, J. A. Bergwerff, P. Barnes and B. M. Weckhuysen, *Angew. Chem., Int. Ed.*, 2007, **46**, 8832.
41 L. Espinosa-Alonso, A. A. Lysova, P. de Peinder, K. P. de Jong, I. V. Koptyug and B. M. Weckhuysen, *J. Am. Chem. Soc.*, 2009, **131**, 6525.
42 L. Espinosa-Alonso, M. G. O'Brien, S. B. M. Jacques, A. M. Beale, K. P. de Jong, P. Barnes and B. M. Weckhuysen, *J. Am. Chem. Soc.*, 2009, **131**, 16932.
43 P. Kubanek, O. Busch, S. Thomson, H. W. Schmidt and F. Schüth, *J. Comb. Chem.*, 2004, **6**, 420.
44 S. J. Taylor and J. P. Morken, *Science*, 1998, **280**, 267.
45 C. M. Snively, G. Oskarsdottir and J. Lauterbach, *Angew. Chem., Int. Ed.*, 2001, **40**, 3028.
46 O. M. Busch, W. Brijoux, S. Thomson and F. Schuth, *J. Catal.*, 2004, **222**, 174.
47 F. Schüth, *J. Phys. Chem.*, 1992, **96**, 7493.
48 L. Karwacki, M. H. F. Kox, D. A. M. de Winter, M. R. Drury, J. D. Meeldijk, E. Stavitski, W. Schmidt, M. Mertens, P. Cubillas, N. John, A. Chan, N. Kahn, S. R. Bare, M. Anderson, J. Kornatowski and B. M. Weckhuysen, *Nat. Mater.*, 2009, **8**, 959.
49 F. Schüth, D. Demuth, B. Zibrowius, J. Kornatowski and G. Finger, *J. Am. Chem. Soc.*, 1994, **116**, 1090.
50 G. Müller, J. Budis, G. Eder-Mirth, J. Kornatowski and J. A. Lercher, *J. Mol. Struct.*, 1997, **410–411**, 173.
51 W. P. J. H. Jacobs, D. G. Demuth, S. A. Schunk and F. Schuth, *Microporous Mater.*, 1997, **10**, 95.
52 S. C. Popescu, S. Thomson and R. F. Howe, *Phys. Chem. Chem. Phys.*, 2001, **3**, 111.
53 E. Lehmann, C. Chmelik, H. Scheidt, S. Vasenkov, B. Staudte, J. Karger, F. Kremer, G. Zadrozna and J. Kornatowski, *J. Am. Chem. Soc.*, 2002, **124**, 8690.
54 C. Chmelik, A. Varmla, L. Heinke, D. B. Shah, J. Karger, F. Kremer, U. Wilczok and W. Schmidt, *Chem. Mater.*, 2007, **19**, 6012.
55 C. Chmelik, J. Kaerger, M. Wiebcke, J. Caro, J. M. van Baten and R. Krishna, *Microporous Mesoporous Mater.*, 2009, **117**, 22.
56 C. Chmelik, F. Hibbe, D. Tzoulaki, L. Heinke, J. Caro, J. Li and J. Kärger, *Microporous Mesoporous Mater.*, 2010, **129**, 340.
57 C. Chmelik, H. Bux, J. Caro, L. Heinke, F. Hibbe, T. Titze and J. Kärger, *Phys. Rev. Lett.*, 2010, **104**, 085902.
58 M. Nowotny, J. A. Lercher and H. Kessler, *Zeolites*, 1991, **11**, 454.
59 E. Stavitski, M. H. F. Kox, I. Swart, F. M. F. de Groot and B. M. Weckhuysen, *Angew. Chem., Int. Ed.*, 2008, **47**, 5637.
60 M. H. F. Kox, E. Stavitski, J. C. Groen, J. Pérez-Ramírez, F. Kapteijn and B. M. Weckhuysen, *Chem.–Eur. J.*, 2008, **14**, 1718.
61 I. L. C. Buurmans, E. A. Pidko, J. M. de Groot, E. Stavitski, R. A. van Santen and B. M. Weckhuysen, *Phys. Chem. Chem. Phys.*, 2010, **12**, 7032.
62 L. Karwacki, E. Stavitski, M. H. F. Kox, J. Kornatowski and B. M. Weckhuysen, *Angew. Chem., Int. Ed.*, 2007, **46**, 7228.
63 E. Stavitski, M. H. F. Kox, I. Swart, F. M. F. de Groot and B. M. Weckhuysen, *Angew. Chem., Int. Ed.*, 2008, **47**, 3543.
64 E. Stavitski, E. A. Pidko, M. H. F. Kox, E. J. M. Hensen, R. A. Van Santen and B. M. Weckhuysen, *Chem.–Eur. J.*, 2010, **16**, 9340.
65 M. H. F. Kox, K. F. Domke, J. P. R. Day, G. Rago, E. Stavitski, M. Bonn and B. M. Weckhuysen, *Angew. Chem., Int. Ed.*, 2009, **48**, 8990.
66 M. H. F. Kox, A. Mijovilovich, J. J. H. B. Sättler, E. Stavitski and B. M. Weckhuysen, *ChemCatChem*, 2010, **2**, 564.
67 K. Ataka, T. Kottke and J. Heberle, *Angew. Chem., Int. Ed.*, 2010, **49**, 5416.
68 B. Hulsken, R. Van Hameren, J. W. Gerritsen, T. Khoury, P. Thordarson, M. J. Crossley, A. E. Rowan, R. J. M. Nolte, J. A. A. W. Elemans and S. Speller, *Nat. Nanotechnol.*, 2007, **2**, 285.
69 A. Kudelski, *Surf. Sci.*, 2009, **603**, 1328.
70 W. Zhang, B. S. Yeo, T. Schmid and R. Zenobi, *J. Phys. Chem. C*, 2007, **111**, 1733.
71 C. Fokas and V. Deckert, *Appl. Spectrosc.*, 2002, **56**, 192.
72 J. S. Samson, G. Wollny, E. Brundermann, A. Bergner, A. Hecker, G. Schwaab, A. D. Wieck and M. Havenith, *Phys. Chem. Chem. Phys.*, 2006, **8**, 753.